AFRL-RX-WP-TP-2008-4046

DEEP DEFECT DETECTION WITHIN THICK MULTILAYER AIRCRAFT STRUCTURES CONTAINING STEEL FASTENERS USING A GIANT-MAGNETO RESISTIVE (GMR) SENSOR (PREPRINT)

Ray T. Ko and Gary J. Steffes

University of Dayton Research Institute

OCTOBER 2007

AIR FORCE RESEARCH LABORATORY
MATERIALS AND MANUFACTURING DIRECTORATE
WRIGHT-PATTERSON AIR FORCE BASE, OH 45433-7750
AIR FORCE MATERIEL COMMAND
UNITED STATES AIR FORCE

REPORT DOCUMENTATION PAGE

Form Approved
OMB No. 0704-0188

1. REPORT DATE *(DD-MM-YY)*
October 2007

2. REPORT TYPE
Conference Paper Preprint

3. DATES COVERED *(From - To)*
01 April 2006 – 31 March 2007

4. TITLE AND SUBTITLE
DEEP DEFECT DETECTION WITHIN THICK MULTILAYER AIRCRAFT STRUCTURES CONTAINING STEEL FASTENERS USING A GIANT-MAGNETO RESISTIVE (GMR) SENSOR (PREPRINT)

5a. CONTRACT NUMBER
F33615-03-C-5219

5b. GRANT NUMBER

5c. PROGRAM ELEMENT NUMBER
62102F

6. AUTHOR(S)
Ray T. Ko (University of Dayton Research Institute)
Gary J. Steffes (AFRL/RXLP)

5d. PROJECT NUMBER
4349

5e. TASK NUMBER
41

5f. WORK UNIT NUMBER
43494107

7. PERFORMING ORGANIZATION NAME(S) AND ADDRESS(ES)

University of Dayton Research Institute
Structural Integrity Division
300 College Park
Dayton, OH 45469-0120

Nondestructive Evaluation Branch (AFRL/RXLP)
Metals, Ceramics & Nondestructive Evaluation Division
Materials and Manufacturing Directorate
Wright-Patterson Air Force Base, OH 45433-7750
Air Force Materiel Command, United States Air Force

8. PERFORMING ORGANIZATION REPORT NUMBER

9. SPONSORING/MONITORING AGENCY NAME(S) AND ADDRESS(ES)
Air Force Research Laboratory
Materials and Manufacturing Directorate
Wright-Patterson Air Force Base, OH 45433-7750
Air Force Materiel Command
United States Air Force

10. SPONSORING/MONITORING AGENCY ACRONYM(S)
AFRL/RXLP

11. SPONSORING/MONITORING AGENCY REPORT NUMBER(S)
AFRL-RX-WP-TP-2008-4046

12. DISTRIBUTION/AVAILABILITY STATEMENT
Approved for public release; distribution unlimited.

13. SUPPLEMENTARY NOTES
The U.S. Government is joint author of this work and has the right to use, modify, reproduce, release, perform, display, or disclose the work. PAO Case Number: AFRL/WS 07-2128, 12 Sep 2007.
Paper contains color.

14. ABSTRACT
Defect detection within thick multilayer structures containing steel fasteners is a challenging task in eddy current testing due to the magnetic permeability of the fasteners and overall thickness of the structure. To address these issues, a magnet is applied to the fasteners during the inspection to reduce the noise caused by the permeability. Using a GMR sensor coupled with a lock-in amplifier to increase eddy current sensitivity, data is obtained and at low frequencies. After developing a basic signal processing algorithm, the experimental results show this system can detect second layer defects occurring 10-mm below the surface of an aluminum structure with steel fasteners.

15. SUBJECT TERMS
GMR, eddy current, permeability, low frequency

16. SECURITY CLASSIFICATION OF:			17. LIMITATION OF ABSTRACT:	18. NUMBER OF PAGES	19a. NAME OF RESPONSIBLE PERSON (Monitor)
a. REPORT	b. ABSTRACT	c. THIS PAGE			Gary J. Steffes
Unclassified	Unclassified	Unclassified	SAR	14	19b. TELEPHONE NUMBER *(Include Area Code)* N/A

Standard Form 298 (Rev. 8-98)
Prescribed by ANSI Std. Z39-18

DEEP DEFECT DETECTION WITHIN THICK MULTILAYER AIRCRAFT STRUCTURES CONTAINING STEEL FASTENERS USING A GIANT-MAGNETO RESISTIVE (GMR) SENSOR

Ray T. Ko, Gary J. Steffes[1]

[1] Metals, Ceramics, and NDE Division, Air Force Research Laboratory,
Wright-Patterson Air Force Base, Dayton, Ohio 45433

Structural Integrity Division, University of Dayton Research Institute,
300 College Park, Dayton, Ohio 45469-0120

Abstract. Defect detection within thick multilayer structures containing steel fasteners is a challenging task in eddy current testing due to the magnetic permeability of the fasteners and overall thickness of the structure. To address these issues, a magnet is applied to the fasteners during the inspection to reduce the noise caused by the permeability. Using a GMR sensor coupled with a lock-in amplifier to increase eddy current sensitivity, data is obtained and at low frequencies. After developing a basic signal processing algorithm, the experimental results show this system can detect second layer defects occurring 10-mm below the surface of an aluminum structure with steel fasteners.

Keywords: GMR, eddy current, permeability, low frequency
PACS: 81.70.Ex

INTRODUCTION

There are many applications throughout the aerospace industry that have aluminum structures assembled with steel fasteners. Steel fasteners are used due to their lower cost and high strength properties. Unfortunately, these dissimilar metals cause Non-Destructive Evaluation (NDE) difficulties when the health of these structures needs to be assessed using conventional eddy current methods.

NDE becomes very challenging when structures with steel fasteners are thicker, more complex, and involve the evaluation of several layers of materials beneath the surface. Two reasons for this difficulty are: the magnetic permeability of the steel fasteners in the structure, and the overall sensitivity of the eddy current test instrumentation. The variation of permeability in steel fasteners is a source of background noise in defect detection using eddy currents. In addition, the sensitivity of eddy current inspections in thick and highly conductive materials is degraded when using lower frequencies appropriate for thick and complex structures.

To address these issues, a magnet has been applied to the fasteners to reduce the noise caused by the permeability. In addition, a GMR sensor coupled with a lock-in amplifier was used to obtain data and to increase the eddy current sensitivity at low frequencies. Experimental results of a test specimen with defects in both the faying surface of the first layer and the faying surface of the second layer will be shown using a test setup that addresses the issues above.

TEST SPECIMEN

The test specimen is composed of two layers of 7075-T7351 aluminum, a 6.3 mm thick first layer and a 3.7 mm thick second layer, assembled with two rows of countersunk steel fasteners. The specimen contains individual EDM notches representing fatigue cracks initiating from individual fastener holes. The EDM notches are various lengths among the fastener holes and located on the bottom of the first layer (in first row), as well as, the bottom of the second layer (the second row). A schematic of the specimen cross section at a fastener location is shown in Figure 1. The EDM notches geometries were corner notches at the fastener holes with 3:1 aspect ratios. In other words, a single EDM notch could have a 7.5 mm length along the faying surface of a layer with a 2.5 mm length along the bore based on the aspect ratio. Finally, there are also fastener holes without any notches in each row to provide a reference. This test specimen was provided to the USAF courtesy of the Canadian Air Force.

LABORATORY EXPERIMENT

The overall laboratory setup is shown in Figure 2. The electromagnetic sensor uses a drive coil for transmitting a magnetic field and a GMR sensor for detecting the magnetic field response. The coil is a bobbin coil with the inner diameter 7.5 mm and the outer diameter 20 mm. The coil height is also 7.5 mm. The wire used for this coil is 34 AWG wire. Lastly, the commercially available GMR sensor is embedded inside the coil.

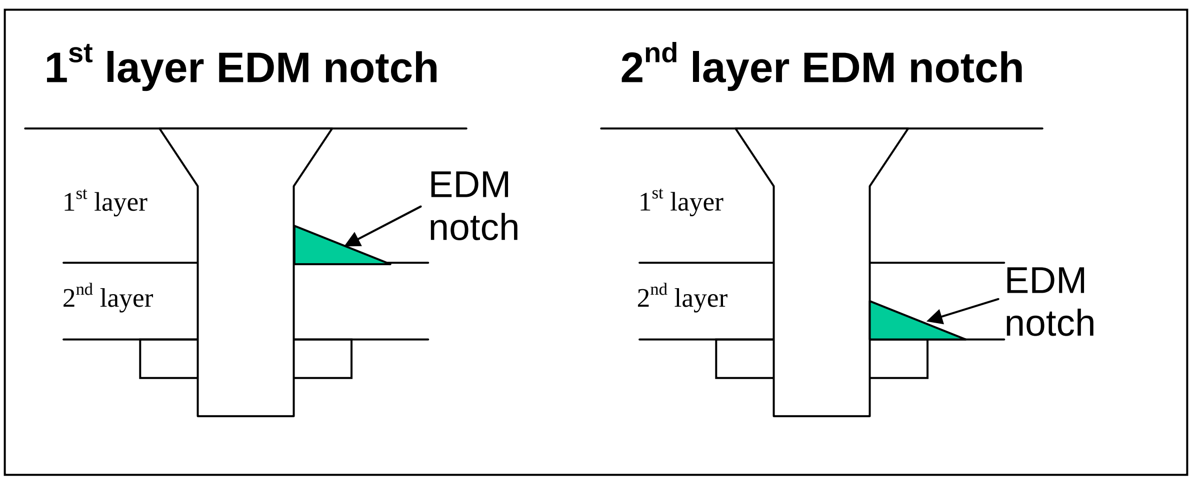

FIGURE 1. A schematic shows the cross section view of a fastener hole showing EDM notches in the 1st layer and 2nd layer, respectively. The ferromagnetic fastners are coutersunk and flush with the top surface.

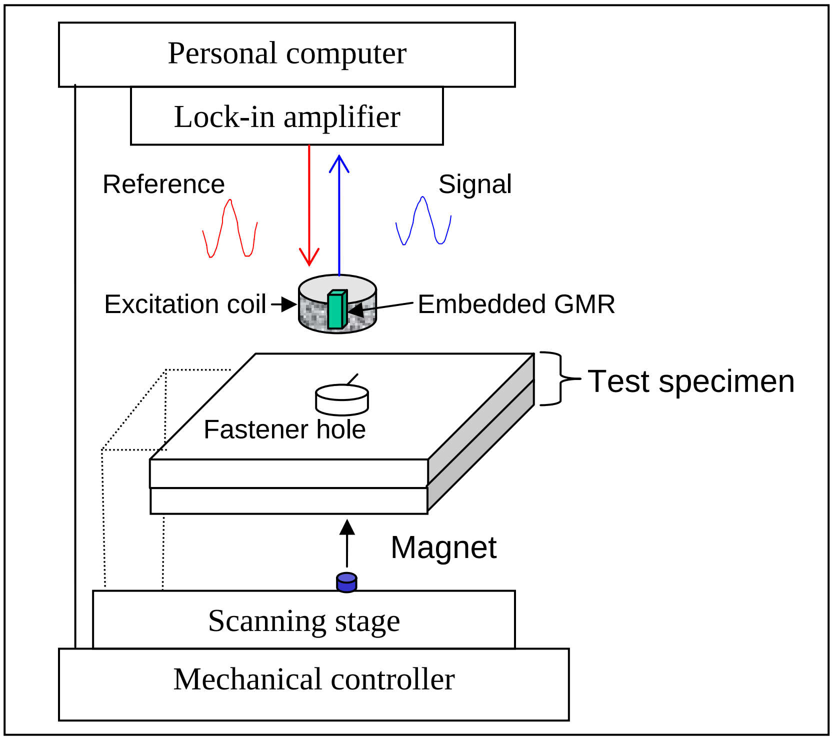

FIGURE 2. A schematic showing the laboratory setup for this test to detect an EDM notch initiating from a fastener hole containing a steel fastener.

The detection scheme of the GMR sensor is based on the direction change of the magnetic field due to the presence of flaws in a simple plate. Thus, the sensitive axis of the GMR sensor is parallel to the specimen. However, the sensitivity axis of the GMR in this setup is rotated 90-degrees to avoid issues due to non-constant edge signals from fastener holes causing strong interference patterns.

For this feasibility study, a magnet of 5 Kilo-Gauss is placed 200 mm below the specimen directly underneath the fastener on the top surface of the scanning stage (see Figure 2). This permanent magnet provides a strong DC bias to re-align the magnetic domains in the fasteners beyond the saturation range of a typical B-H curve which makes this ferromagnetic material respond like a non-ferromagnetic material for this NDE test setup. Special considerations were taken in this study not to saturate the GMR chips within the sensor.

A simple GMR sensor usually contains two pairs of GMR chips in a bridge configuration. The GMR measurement is differential and made by comparing the response of the lone pair exposed to the magnetic field to that of the reference pair which are covered with mild permalloy materials shielded from the intense magnetic field.

The instrumentation includes a lock-in amplifier which excites the coil at a sinusoidal reference signal and compares it to the signal received from the GMR sensor to determine the phase and magnitude. The data acquisition for this test is taken from scanned area of a 50-mm square with a step size of 1-mm square. At each measurement location, both phase and magnitude measurements were recorded in the computer. The generated image plots, shown below, are based upon the phase information from the lock-in amplifier. Scan frequencies of 130 Hz were used to detect cracks at the backside of the second layer (10 mm below top surface), and 340 Hz were used to detect cracks at the backside of the top layer (6.7 mm below top surface).

LOCK-IN PHASE EXPERIMENT

While it is possible to output a GMR signal to an oscilloscope, an alternative way to drive a coil and measure the output is to use a lock-in amplifier. The lock-in amplifier system is based on the comparison of a known reference input signal to the coil with the output signal from the GMR sensor at a given frequency. The magnitude of the output signal is a DC signal and proportional to the product after filtered. Using a second device inside the lock-in amplifier, the phase difference between the reference input and the GMR output signals can also be monitored, see Figure 3. The information from this phase difference was used to generate the following phase image maps. The lock-in instrument used in this setup contains two channels that displays both magnitude and phase measurements.

CRACK DETECTION

The typical phase image map derived from this testing is shown on the left side of Figure 4. The crack detection is made by processing the waveforms and making signal comparisons between both sides of the fastener along the horizontal and vertical axes, respectively. This is shown on the right side of Figure 4. For example, by slicing the image through the center at each axial location, two waveforms can be obtained from each of the horizontal and vertical directions. Each waveform contains information regarding the magnetic field response at +/- 90° locations with respect to the fastener shank. These locations are compared by folding the waveform about the center and making a simple subtraction of signals from both sides. This self-differential technique is then applied to the fastener data to detect flaws in the specimen. In the case of no defect, the resultant subtracted signals for each axis is close to zero. It provides a rapid discrimination of flaw detection while another type of analysis around the fastener hole can also be made to provide more detailed information [1].

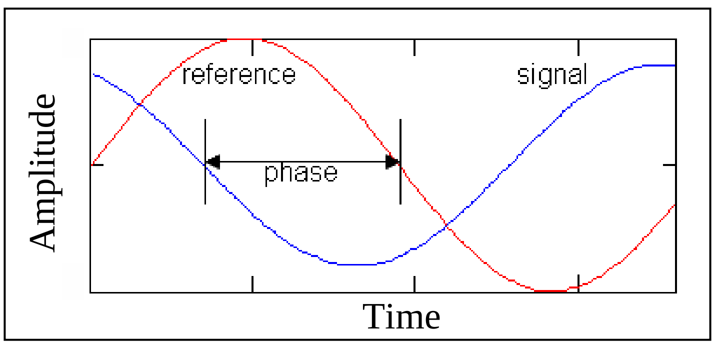

FIGURE 3. The phase between an input signal and the reference signal in a lock-in phase measruement.

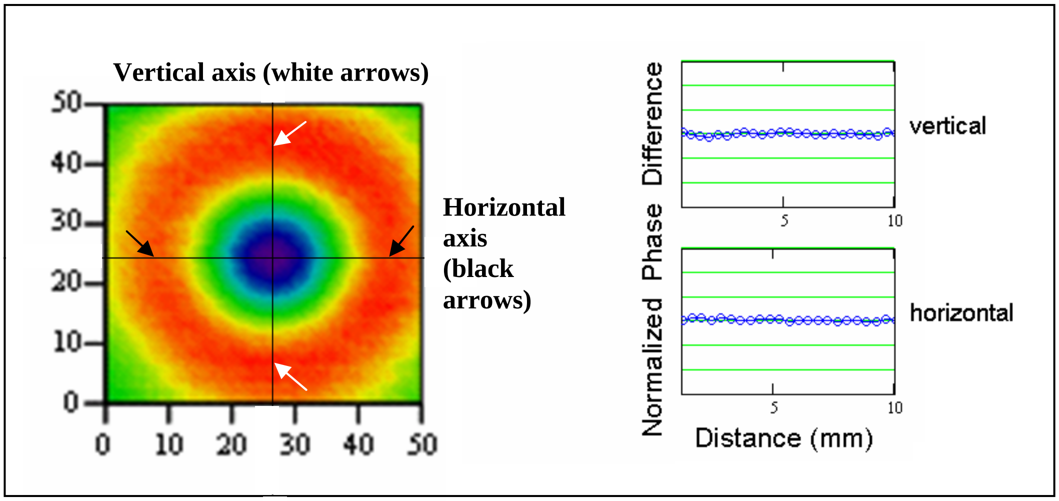

FIGURE 4. A typical phase image from a GMR sensor response from a fastener and hole. This particular scan was in an area with no defects. Edge signals at both axes are compared for defect detection. The axial lines show the locations that derive the normalized phase difference plots on the right, and the arrows show the approximate locations where waveform differences tend to show up in the normalized phase difference plots.

2ND LAYER TEST RESULTS (Scan Frequency 130Hz)

Figure 5 shows the phase image map, at left, and processed waveforms after signal comparison, at right. This particular scan is of a fastener area with a 10-mm notch under 10-mm thickness of aluminum in the vertical direction. Based on the phase image map, the signal perturbation due to the notch is not significant enough to draw attention. However in the processed waveform, the flaw indication becomes visible.

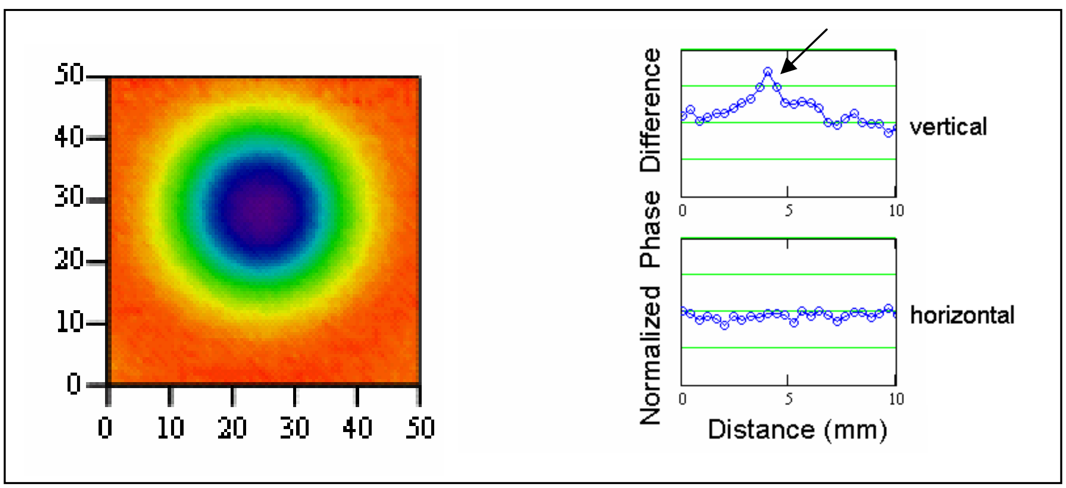

FIGURE 5. Phase image map and processed waveforms after signal comparison showing the detection of a 10-mm notch under 10-mm of aluminum, see arrow.

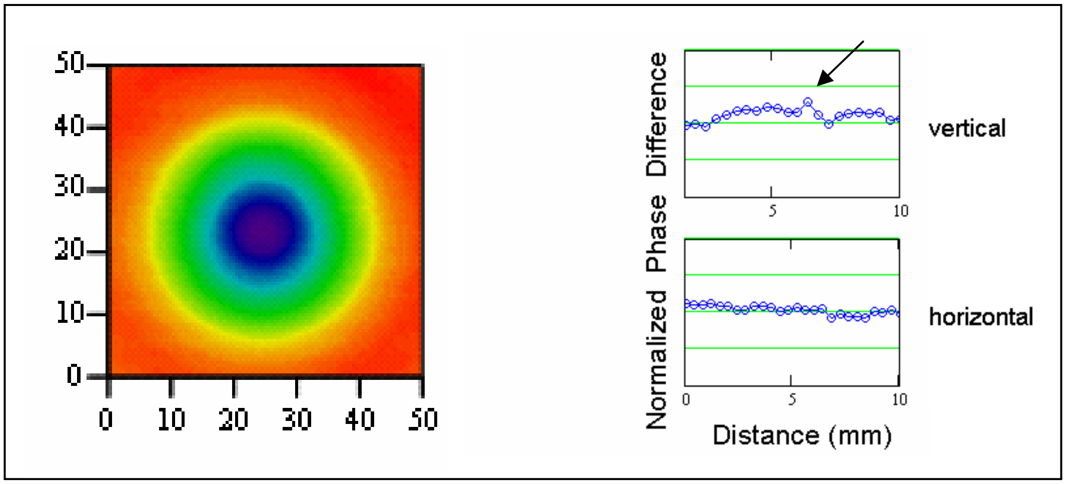

FIGURE 6. Phase image map and processed waveforms after signal comparison showing the detection of a 7.5-mm notch under 10-mm of aluminum, see arrow.

Figure 6 shows an additional phase image map, at left, and the processed waveforms after signal comparison, at right. This particular scan is of a fastener area with a 7.5-mm notch under 10-mm thickness of aluminum. Similar to the phase image map in Figure 5, the perturbation due to the notch is not significant enough to draw attention, but in the processed waveform, the flaw indication becomes more visible.

1ST LAYER TEST RESULTS (Scan Frequency 340Hz)

The scan area of the following phase image map and processed waveforms, shown in Figure 7, contained a 10-mm notch under 6.3-mm of aluminum, and also was detected as a result of the vertical axial comparison. From the phase image itself, the perturbation due to the notch is difficult to see, but in the processed waveform, the flaw indication becomes much more visible.

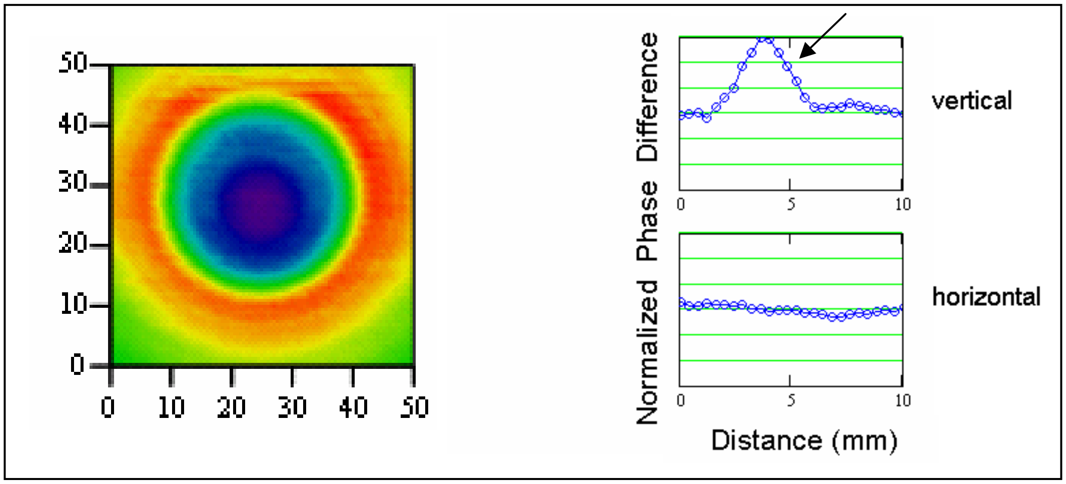

FIGURE 7. Phase image map and processed waveforms after signal comparison showing the detection of a 10-mm notch under 6.3-mm of aluminum, see arrow.

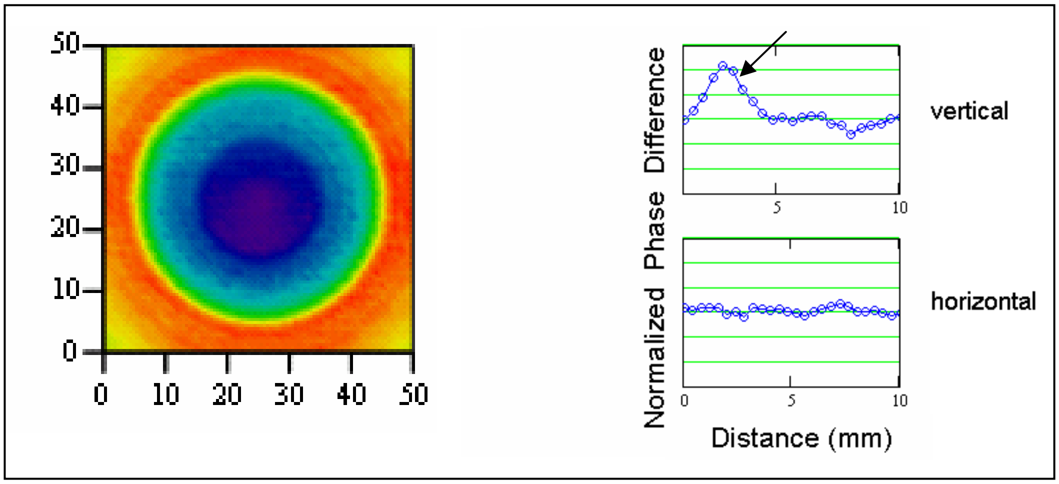

FIGURE 8. Phase image map and processed waveforms after signal comparison showing the detection of a 7.5-mm notch under 6.3-mm of aluminum, see arrow.

The scan area of the following phase image map and processed waveforms, shown in Figure 8, contained a 7.5-mm notch under 6.3-mm of aluminum, and also was detected by the same method. Once again, the perturbation due to the notch is difficult to see in the phase image map, but after waveform processing, the flaw indication becomes much more visible.

As expected, the signal responses due to the notches shown in Figures 7 and 8 had much higher amplitudes than the signal responses shown in Figures 5 and 6. This means that the notches in the first layer yielded a much stronger signal output for this test than those in the second layer. Additionally, the signal responses from larger notches were stronger than those from smaller notches. This provides a basis for further work that could improve the spatial definition and notch characterization of GMR signals.

CONCLUSIONS

Several issues arise when using conventional eddy current NDE to detect defects within thick multilayer structures containing steel fasteners. Using a GMR sensor, a lock-in amplifier, a magnet, and a differential algorithm, the issues of magnetic permeability in fasteners and material thickness that prevent defect detection can be addressed. The results of this study showed initial success in detecting large notch sizes under thick aluminum structure that contained steel fasteners, specifically 7.5 and 10-mm long corner notches in fastener holes under 6.7 and 10-mm of aluminum. During this study, several observations were made regarding the signal amplitude that could ultimately translate into improved spatial definition and characterization of fatigue cracks in thick complex structures.

ACKNOWLEDGEMENT

This work was performed on-site in the Nondestructive Evaluation Branch of the Air Force Research Laboratory (AFRL/MLLP) at Wright Patterson AFB, OH, under Air Force contract # F33615-03-C-5219.

The authors would also like to acknowledge Captain D.J. Butcher of the Aerospace and Telecommunications Engineering Support Squadron of the Canadian Air Forces Base Trenton for providing the specimen for this test.

REFERENCE

1. N. Schehl, W. Hoppe, R. Ko, A. Berens, "Evaluation of Intergranular Corrosion Detection Method on the Structural Repair of Aging Aircraft Program," proceedings of the Fifth Joint NASA/FAA/DoD conference on Aging aircraft, Orlando, FL, Sept. 10-13, (2001).